HHS Public Access

Author manuscript

Nano Lett. Author manuscript; available in PMC 2019 August 26.

Published in final edited form as:

Nano Lett. 2017 November 08; 17(11): 7045–7054. doi:10.1021/acs.nanolett.7b03734.

Biologically Inspired Design of Nanoparticle Artificial Antigen-Presenting Cells for Immunomodulation

John W. Hickey[†,‡,ǁ,⊥], **Fernando P. Vicente**[†], **Gregory P. Howard**[†,⊥], **Hai-Quan Mao**[ǁ,⊥,#], **Jonathan P. Schneck**[*,‡,§,⊥,∇]

[†]Department of Biomedical Engineering, School of Medicine

[‡]Institute for Cell Engineering, School of Medicine

[§]Department of Pathology, School of Medicine

[ǁ]Translational Tissue Engineering Center

[⊥]Institute for Nanobiotechnology

[#]Department of Materials Science and Engineering, Whiting School of Engineering

[∇]Department of Medicine, School of Medicine, Johns Hopkins University, Baltimore, Maryland 21231, United States

Abstract

Particles engineered to engage and interact with cell surface ligands and to modulate cells can be harnessed to explore basic biological questions as well as to devise cellular therapies. Biology has inspired the design of these particles, such as artificial antigen-presenting cells (aAPCs) for use in immunotherapy. While much has been learned about mimicking antigen presenting cell biology, as we decrease the size of aAPCs to the nanometer scale, we need to extend biomimetic design to include considerations of T cell biology—including T-cell receptor (TCR) organization. Here we describe the first quantitative analysis of particle size effect on aAPCs with both Signals 1 and 2 based on T cell biology. We show that aAPCs, larger than 300 nm, activate T cells more efficiently than smaller aAPCs, 50 nm. The 50 nm aAPCs require saturating doses or require artificial magnetic clustering to activate T cells. Increasing ligand density alone on the 50 nm aAPCs did not increase their ability to stimulate CD8+ T cells, confirming the size-dependent phenomenon. These data support the need for multireceptor ligation and activation of T-cell receptor (TCR) nanoclusters of similar sizes to 300 nm aAPCs. Quantitative analysis and modeling of a

[*]Corresponding Author: jschnec1@jhmi.edu. Phone: 410-614-4589.

Author Contributions

J.W.H., H.Q.M., and J.P.S. designed the studies and wrote the manuscript. J.W.H. and F.P.V. performed the experiments. G.P.H. performed TEM imaging of particles. J.W.H., F.P.V., H.Q.M., and J.P.S. analyzed the data.

Supporting Information

The Supporting Information is available free of charge on the ACS Publications website at DOI: 10.1021/acs.nanolett.7b03734. Supplemental Tables 1–2, Supplemental Figures S1–12, and materials and methods (PDF)

The authors declare the following competing financial interest(s): Under a licensing agreement between NexImmune and The Johns Hopkins University, Jonathan Schneck is entitled to a share of royalty received by the university on sales of products described in this article. He was also a founder of NexImmune and owns equity in the company and he serves as a member of NexImmune's Board of Directors and scientific advisory board. The terms of these arrangements have been reviewed and approved by The Johns Hopkins University in accordance with its conflict of interest policies.

nanoparticle system provides insight into engineering constraints of aAPCs for T cell immunotherapy applications and offers a case study for other cell-modulating particles.

Graphical Abstract

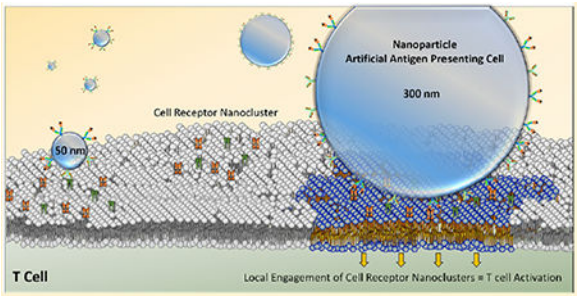

Keywords

Artificial antigen presenting cell; immunotherapy; nanoparticle; CD8+ T cell; particle size; receptor clustering

Engineering the body's immune system is an attractive approach to treating and preventing diseases. CD8+ T cells are good targets for implementing precision immunomodulation against pathogens and tumors with antigen-specificity. Furthermore, the memory response of these cells gives this approach potential long-term durability. As a consequence, controlling CD8+ T cell responses is one of the goals of adoptive cell therapy (ACT) for cancer immunotherapy[1] However, the activation of CD8+ T cells for therapy is costly and technically challenging. One of the main hurdles of ACT is generating enough functional antigen presenting cells (APCs) to stimulate antitumor CD8+ T cells. Endogenous APCs from cancer patients are frequently dysfunctional due to immunosuppression from the tumor microenvironment. Additionally, ACT often requires multiple leukophoreses; and yet the outcomes vary significantly from patient to patient.[2–4]

To bypass cell-based endogenous APCs, we have developed particle-based artificial antigen presenting cells (aAPCs).[5,6] These particles are coated with the two stimulatory signals needed for effective CD8+ T cell activation—peptide loaded major histocompatibility complex (pMHC) (Signal 1) and costimulatory anti-CD28 (Signal 2) (Figure 1a). Using a particle-based system offers a convenient off-the-shelf product and cellular replacement for ACT, ultimately leading to the control and standardization of CD8+ T cell activation.

Furthermore, particle-based aAPC properties can be engineered to more efficiently activate and modulate antigenspecific T cells.[7] For example, the shape of the particle can be changed to promote increased attachment with the T cells;[8,9] biodegradable particles can be used to modulate T cells in vivo,[10] and particles can encapsulate and deliver other cell modulators such as cytokines[11,12] and can be used in combination therapies such as with checkpoint blockade molecules.[13]

The particle size and stimulatory ligand surface density are important determinants that influence the interaction of particles and cells.[14] Our original designs of aAPCs were based on particles of several microns in diameter—chosen to mimic the endogenous APCs.[5] However, using micron-sized particles presents a challenge for in vivo application due to the issue of potential embolization. Nanoparticles offer enhanced biodistribution to reach lymph nodes if injected subcutaneously[15] or to reach tumors if injected intravenously.[16] More recently, we have demonstrated that nanoparticle (NP) aAPCs with an average size of 50 nm can provide therapeutic benefit in adoptive cell transfer models.[17,18] Also, others have recently employed nanoparticles with only pMHC conjugated (no costimulation) to induce a regulatory response instead of activating T cells for autoimmune applications.[19] Here the size was also explored, but in a limited size range between 4 and 20 nm.[20] Therefore, the detailed effect of particle size on T-cell activation efficiency has not yet been well-defined.

Differences in particle dimensions could have implications due to nanometer-scale structures of signaling molecules at the surfaces of T cells and APCs. It has been shown, for example, that T cell receptors (TCRs) are preclustered into protein islands of around 35–70 nm in radius and 300 nm at the longest length scale with 7–30 TCRs per island.[21,22] Furthermore, pMHC patches have also been observed on APCs with radii from 70 to 600 nm and about 25–125 pMHC per patch.[23] Therefore, we hypothesized that nanoparticles with similar size dimensions to TCR islands and pMHC patches would result in more effective engagement and activation of T cells.

Another parameter important to T cell activation is stimulatory ligand density. CD4+ T cells are insensitive to activation when the density of Signal 1 (pMHC) is too low. Interestingly, for antigen-independent stimulation with anti-CD3, the activation threshold was a maximum linear distance of 60–70 nm;[24,25] however, the linear distance was close to 115 nm for pMHC class II molecules.[26] Thus, nanometer scale distances and ligand densities have clear implications for nanoparticle aAPC design and may offer novel insights to how the influence of ligand density is impacted by being attached to a mobile platform.

In this study, we tailored size, stimulatory ligand density, and concentration of particle aAPCs to modulate T cell activation (Figure 1b). Our strategy is based from an effort to see whether design considerations of T cell biology, such as TCR organization, will improve the efficiency of nanosized aAPCs. These findings will provide important guidance to control the efficiency of T cell stimulation using nanoparticle-based aAPCs for immunotherapeutic applications.

We prepared aAPCs from superparamagnetic iron oxide nanoparticles (SPIONs). SPIONs can be formulated to have a defined size range and can be manipulated in a magnetic field. We conjugated chimeric pMHC-Ig loaded with model antigen SIY (Signal 1) and anti-CD28 antibody (Signal 2) at a 1:1 molar ratio to particles of different average sizes—50, 300, 600, and 4500 nm. All aAPC particles were stable postconjugation and maintained distinct size populations (Figure 1c, Supplemental Figure 1, Supplemental Table 1). All nanoparticle aAPCs across sizes and densities had between —1 and −10 mV zeta potential when measured in PBS at a pH of 7.4 (Figure 1d). While the density of stimulatory signals between different sized aAPCs varied slightly, for the 50 nm aAPCs we were able to make a

high (HD) and low density (LD) version where the ligand density differed by 100-fold (Figure 1e, Supplemental Figure 1, Supplemental Table 1).

Using the panel of well-defined, nanoparticle-based aAPCs, we found a size-dependent association with T cell activation. At a concentration of 2 pM of particle-bound Signal 1, Kb-SIY, we observed a significant decrease in the ability for 50 nm aAPCs to stimulate their cognate 2C CD8+ T cells compared to particles larger than 300 nm (Figure 2a). We controlled for the total number of bound pMHCs in all experiments because this parameter has been a critical factor in T cell activation in past studies, and not the number of aAPCs.[27] Although we kept the surface ligand concentration constant in each condition, a greater number of smaller aAPCs were added than larger aAPCs because larger aAPCs had more surface-bound ligand per particle. At 2 pM, 50 nm aAPCs only produced a 5-fold CD8+ T cell expansion, which statistically differed from all larger particles. All particles larger than 300 nm produced around 12-fold T cell expansion—a value indicative of a robust stimulation of T cells for a 7 day culture period—and were not statistically different from one another. The differences between 50 nm and larger aAPCs to provide stimulation were consistent with the need to engage local islands of Signals 1 (pMHC) and 2 (aCD28) greater than 50 nm in diameter for effective CD8+ T cell stimulation.

To show this size-dependent effect is independent of particle preparation, we formulated aAPCs from another set of iron-oxide particles of 50, 300, and 600 nm diameters (Supplemental Figure 2, Supplemental Table 1). We observed ineffective stimulation with the 50 nm aAPCs when compared to the larger aAPCs (Supplemental Figure 3a). Importantly, we did not observe any activation by aAPCs with noncognate pMHC (Kb-TRP2) and anti-CD28 of any size (Supplemental Figure 3b). Repeating this experiment in another particle system substantiated the evidence of a size-dependent effect observed with nanoparticle aAPCs.

These first two experiments examined proliferation as a functional readout for T cell activation; however, early signaling events may provide additional insight into the mechanism of the aAPC-T cell interaction. To do so we stimulated T cells for 30 min and examined MAPK signaling by staining for phosphorylated ERK1/2 (pERK). Similar to our proliferation results, we observed robust early signaling by 300 nm and larger aAPCs as indicated by the mean fluorescent intensity (MFI) of pERK, yet 50 nm aAPCs did not produce a detectable signal (Figure 2b, Supplemental Figure 4a). Others have recently shown that local clusters of TCR-pMHC interactions are necessary both for T cell activation and for effective initial phosphorylation of ERK.[28] This result provided additional support to our hypothesis that 50 nm aAPCs are unable to cluster local TCRs to achieve robust T cell activation.

Another indicator of early, robust T cell activation is through effective mTOR signaling, where phosphorylated ribosomal protein S6 (pS6) is a downstream target of activated mTOR.[29,30] We stained for pS6 after activating the T cells for 30 min, and found consistent results between both proliferation and pERK data. Levels of pS6 for 300 nm and larger aAPCs were significantly higher than those produced by either 50 nm aAPCs or the nonstimulated negative control (Figure 2c, Supplemental Figure 4b). Recently, it has been

shown that effective pS6 staining is correlated to the duration of the APC-T cell contact.[31] Therefore, larger aAPCs may be able to contact CD8+ T cells longer because of greater multivalent binding and thus provides another mechanism to the observed size-dependent effect.

Shorter signaling duration has been associated anergy in CD4+ T cells.[31] We did not expect the aAPCs to induce anergy because we have conjugated a Signal 2, costimulation (anti-CD28) in addition to pMHC, which has been shown to induce activation rather than anergy in T cells.[32,33] Nevertheless, we wanted to confirm whether the reduced activity of CD8+ T cells from 50 nm aAPCs was due to suboptimal signaling or just ineffective engagement of the CD8+ T cell. We first examined TCR downregulation, which is associated with TCR engagement and T cell activation.[34,35] We stimulated T cells with 2 pM dose of the aAPCs and observed a significant decrease in TCR expression for cells stimulated with 300-, 600-, 4500 nm aAPCs, but not 50 nm aAPCs when compared to noncognate aAPCs and no stimulation controls (Figure 2d). Additionally, we probed for a regulatory phenotype at day 7 as defined by other researchers who use pMHC-only (no costimulation) and have induced an immunoregulatory CD8+ T cell response, which are both CD122+ and CD44+.[19,20] After stimulating with aAPCs, we found no significant difference in the percentages between all aAPCs (Supplemental Figure 5). Moreover, we formulated a 300 nm particle with only pMHC (which we term 300 S1), to replicate the type of particle used in previous studies.[19,20] Importantly, here we found that there was a significant increase in the percent of a regulatory phenotype at day 7 (Supplemental Figure 5)—further substantiating evidence for the importance of having both pMHC (Signal 1) and costimulatory anti-CD28 (Signal 2) on the particle for an immune activating response. These data point to ineffective engagement of the CD8+ T cell rather than suboptimal signaling leading to anergy by the 50 nm aAPCs.

To better understand the interaction of different sized particle aAPCs and T cells, we imaged the aAPCs and T cells using transmission electron microscopy (TEM). Interestingly, very few 50 nm aAPCs attached to the T cells, where on average only about one particle attached to a T cell in the 70 nm slice, whereas many more 300 and 600 nm aAPCs attached to the surface of the T cells (Figure 2e). Additionally, the 300 and 600 nm aAPCs were distributed over the surface of the T cell, yet there seemed to be areas where multiple particles attached near each other. These images support both of our proposed mechanisms for why we observe the size-dependent effect—the size of TCR clusters and duration of attachment via increased avidity. More specifically, we observed that the 50 nm aAPCs were not clustered, nor attached well to the T cell compared to the larger 300 and 600 nm aAPCs.

To further probe the size-dependent phenomenon, we asked if we could overcome the restriction with increasing the dose of pMHC and thus total particle numbers. Schematically we are testing that if by adding excess aAPCs, then multiple 50 nm aAPCs could diffuse and engage a single TCR cluster and achieve similar T cell activation, or if clusters need to be ligated by a single larger nanoparticle (Figure 3a). Furthermore, by adding more aAPCs, this may increase the number of aAPCs bound at one time and increase the signaling duration. Indeed, at surface saturating concentrations of 50 nm aAPCs (18 pM of particle-bound Kb-SIY), 50 nm aAPCs were able to stimulate the CD8+ T cells just as well as the larger particles (Figure 3b). All aAPCs produced around 12-fold CD8+ T cell expansion with no

statistical difference between any of the groups. We confirmed that this saturating dose of nanoparticle-based aAPC stimulation resulted in a similar final CD8+ T cell phenotype (surface markers) and functionality (cytokine analysis), further supporting that TCR clusters may be activated by multiple smaller particles, but not necessarily by a single particle 50 nm or less (Supplemental Figure 6a–b).

We extended this finding by quantitating the minimum number of aAPCs required for activation at each aAPC size. Interestingly, this revealed three separate patterns in the number of aAPCs needed to provide effective T cell signaling (Figure 3c). First, the minimum number of 50 nm aAPCs needed to activate T cells is similar to the number of TCRs per T cell, which is reported to be around $0.5–1 \times 10^5$ per T cell.[36] Second, larger aAPCs, 300- and 600 nm, require many fewer aAPCs than the number of TCR per T cell, and much lower than the estimated number of nanoislands per T cell—ca. 15 000, assuming about 30 TCR per island.[21] Third, the 4500 nm aAPCs required even fewer aAPCs—less than one per T cell.

The high number of 50 nm aAPCs required for activation further confirms that there is a need for a surface saturating amount of aAPCs, since nanoparticle aAPCs diffuse through solution, their binding with TCRs will be stochastically distributed over the surface of the CD8+ T cell. Estimating the T cell to have around 50,000 TCRs, to achieve complete nanoisland ligation, all or most TCRs should be bound by 50 nm aAPCs (Supplemental Figure 7a). Furthermore, the need for many fewer 300- and 600 nm aAPCs supports the idea that individual particle aAPCs can bind multiple TCRs in TCR nanoislands to achieve local stimulation with only one particle per island. Finally, the low numbers of 4500 nm aAPCs points to a different signaling mechanism where multiple TCR clusters are bound by a single particle; and multiple T cells can be stimulated by the same particle. The need for a surface saturating amount of 50 nm aAPCs can also be examined by plotting the ratio of particle aAPC surface area to cell surface area (Supplemental Figure 7b). Consequently, this shows that 50 nm nanoparticles need nearly a 1:1 ratio of particle surface area to T cell area to activate T cells, whereas aAPCs larger than 50 nm need less than a 1:5 ratio of particle to T cell surface area.

To connect our findings involving synthetic aAPCs to studies with endogenous APCs, we calculated the average number of available pMHCs per T cell (Figure 3d). Previous studies have reported between 1 and 400 pMHCs are needed to activate a CD8+ T cell.[37–44] While for aAPCs the pMHC is conjugated to a solid scaffold and not within a mobile lipid bilayer with additional signaling molecules, the results seen are consistent with previous reports. We found that the “cell-sized” 4500 nm aAPCs required about 3 pMHCs per T cell. These averages were also similar to numbers found through direct observation of cell-based APCs, where 10 pMHCs were needed to activate a CD8+ T cell and only 3 pMHCs were needed to activate for killing.[42] The 300 and 600 nm aAPCs both required close to 200 pMHCs per T cell, which also falls within the range that has been calculated by indirect averages of endogenous APCs. In contrast, 50 nm aAPCs required more than 10 000 pMHCs per T cell —pointing to the spatial relation or on-rate of the pMHCs when engaged may be important parameters for activation rather than total pMHCs available to a T cell.

Cells are able to dynamically rearrange and cluster receptors on their surface for enhanced function and signaling.[45–47] We sought to mimic receptor clustering of the diffusely bound 50 nm magnetic particles on the surface of the T cell by applying a magnetic field (Figure 4a). Thus, if individually bound TCRs by 50 nm aAPCs can be physically made to cluster using magnetic force, and effective signaling is generated, then this would strengthen our hypothesis of the importance of spatially activating TCRs in clusters.

To artificially cluster TCRs, we placed T cells with 50 nm SPION aAPCs within a static magnetic field.[18] Indeed, artificially clustering 50 nm aAPCs at subsurface saturating amounts stimulates CD8+ T cells to the same level as surface saturating conditions (Figures 3b and 4b). Within a magnetic field 50 nm aAPCs produce approximately a 12-fold, statistically different CD8+ T cell expansion in contrast to the 3-fold expansion without a magnetic field. Artificial clustering of 50 nm aAPCs were comparable to larger aAPCs without artificial clustering. Magnetic clustering of larger aAPCs and surface saturating amounts of 50 nm aAPCs did not further increase CD8+ T cell stimulation, suggesting there is no added benefit to the magnetic field other than providing artificial clustering of diffuse 50 nm particles (Figure 4c).

This result demonstrated that artificial clustering of Signals 1 (pMHC) and 2 (anti-CD28) improved signal activation, suggesting a particle size-dependent signaling effect that is linked with stimulatory signaling molecule clusters. However, taking a reductionist approach and modeling the surfaces of the particle and the T cells as spheres, we determined that a confounding variable is the number of ligands available from particle aAPCs to interact with T cells (Figure 5a, Supplemental Figure 8a–b, Supplemental Table 1). Even if there are similar densities of ligands for particles of different sizes, differences in geometry can lead to differences in number of ligands actually available to engage T cells. We calculated the number of available ligands for each spherical particle at the initial contact (Figure 5a). As the particle size decreases, there is an increase in particle curvature and a decrease in ligands available to interact with T cells.

To decouple the effect of multiple-ligands per TCR nanocluster and stimulation signal cluster size, we prepared 50 nm aAPCs with a higher density of Signals 1 and 2 (HD 50 nm). HD 50 nm aAPCs have the same effective radius (r_{eff}) as their 50 nm counterparts (Supplemental Figure 8a) but a shorter distance between ligands—thus, presenting comparable numbers of effective stimulatory molecules as larger aAPCs (Figure 5a). Using these HD 50 nm aAPCs, we confirmed the size-dependent constraints of 50 nm aAPCs as they are also unable to stimulate T cells effectively at 2 pM of particle-bound pMHC in terms of cellular proliferation (Figure 5b) and in early activation events like ERK phosphorylation, mTOR signaling, and TCR downregulation (Supplemental Figure 9a–c). HD 50 nm aAPCs were even less efficient in activating T cells than the regular density 50 nm aAPCs at the 18 pM dose and required a total dose of 90 pM of particle-bound pMHC to produce a similar maximal T cell expansion. This is to be expected as a large number of HD 50 nm aAPCs is still needed to achieve saturation binding of nanoparticles to T cells. Interestingly at the higher dose of 90 pM, HD 50 nm aAPCs produced a greater apparent expansion of T cells than their regular density 50 nm counterpart. This could be due to particle toxicity or to activation-induced T cell death evoked by adding so many regular

density 50 nm aAPCs. Noncognate 50 nm particle aAPCs at the same dose did not cause any additional toxicities as compared to a traditional 4500 nm aAPC stimulation (Supplemental Figure 10a), ruling out toxicity due to particle numbers. Proliferation analysis by CFSE dilution at the 90 pM dose demonstrated effective cell stimulation and division with the 50 nm aAPCs at an earlier time point than that observed with HD 50 nm aAPCs, consequently pointing to activation-induced T cell death (Supplemental Figure 10b–c).

Thus, even with normalized ligand availability, 50 nm aAPCs were less effective than larger aAPCs at stimulating T cells under subsaturating conditions. These findings support the notion that the size of the aAPCs is particularly important in achieving T cell activation rather than differences in ligand availability. This could be explained by TCR density, as it has been reported to be on the order of 1200 TCR/μm^2.[21] Linearly, this translates to about 30 nm spacing between TCRs, which means that even if small particles have a high density of ligand, all available ligands may not be beneficially engaged over the entire surface of the TCR island. Consequently, small particles result in fewer TCR-MHC interactions and fail to result in sustained activation of the TCR island by an individual particle (Figure 5c). In contrast, larger particles can have multivalent binding with nanoclusters leading to a rapid on-rate of local TCRs.[48–51]

To further investigate the relationship between the observed size-dependent effect and potential mechanism of TCR cluster activation, we again used a magnetic field to artificially cluster the HD 50 nm aAPCs at subsaturating concentrations. We observed effective CD8+ T cell stimulation at both the 2 pM and 18 pM concentrations only when the particles were artificially clustered in a magnetic field (Figure 5d). These results further indicate that activation of TCRs in clusters is important for effective T cell activation and agrees with previous studies that demonstrate the importance of pMHC clustering on endogenous APCs for T cell activation.[46]

This study shows that in addition to ligand spacing (Supplemental Figure 11a), the size of the stimulatory island (particle size) is also important for T cell activation. Previous studies with T cells involving TCR nanoarrays have shown a stimulatory molecule spacing requirement for T cell activation of around 70–120 nm.[24–26] We observe differences from this reported trend with 50 nm aAPCs. Even when using 16 nm linear spacing between ligands, we did not observe as effective stimulation as with larger particles with even larger linear distances between ligands (Supplemental Figure 11a).

Since the size of the particle appears to be a driving factor in our findings, we probed how ligand density influenced T cell stimulation with 600 nm aAPCs. Theoretically, 600 nm aAPCs are able to engage multiple receptors with a linear ligand spacing up to about 150 nm (Supplemental Figure 11b). Since this is close to the values reported from TCR nanoarrays, we hypothesized that we would notice a drop-off in T cell activation with ligand densities in this regime. To test this hypothesis, we formulated 600 nm aAPCs with seven different ligand densities (distance between ligands), ranging from 27 to 800 nm, and added these at a 2 pM concentration to CD8+ T cells (Supplemental Table 2).

We observe that for 600 nm aAPCs, the expansion of CD8+ T cells began to decrease substantially at spacing of about 100 nm (Figure 5e, Supplemental Figure 11c), which is similar to values reported for TCR nanoarrays. Therefore, this shows the importance of engineering ligand spacing as well as size of aAPCs for effective T cell activation.

Our ability to provide a mobile stimulatory unit by conjugating the stimulatory ligands to a particle instead of a nanoarray allowed us to probe unique mechanisms of T cell activation. This particle-based aAPC system enables simultaneous control of both the number of stimulatory molecules and the density of these molecules, something that is difficult to achieve with substrate-conjugated signals. Additionally, whereas substrate-conjugated signals allow the study of how T cells might adapt to a fixed stimulation, particle-conjugated signals allow the study of native T cell biology where stimulation signals are also mobile. Another distinction between this and previous studies is that here we study CD8+ T cells, where previous studies have investigated the effect of ligand spacing and density on CD4+ T cells.

This study provides a systematic understanding of how particle aAPC parameters such as particle size, surface ligand density, and concentration collectively influence T cell activation. We demonstrate that aAPCs larger than 300 nm were more effective at activating CD8+ T cells, presumably due to their ability to initiate clustering of pMHC-TCR and costimulatory interactions due to their size. Mechanistically, once particles bind to TCR nanoclusters, larger particles have an enhanced ability to bind other TCRs with pMHCs and CD28 with anti-CD28 leading to multivalent binding of receptors and sustained signaling necessary for T cell activation.[48–51] This is consistent with recent data from (1) immunoregulatory pMHC-only nanoparticles, (2) DNA chimeric antigen receptors, and (3) endogenous antigen presenting cells. For immunoregulatory pMHC-only nanoparticles, higher ligand densities led to the increased activity of the particles and clustered attachment to T cells.[20] Indirectly, we also observed this as noncognate aAPCs (with anti-CD28) prevented full activation of CD8+ T cells cocultured with cognate aAPCs—presumably because they compete for CD28 binding and decrease the ability for multivalent binding (Supplemental Figure 12). For DNA chimeric antigen receptor T cells, it was necessary that a small group of the receptors be clustered by the counterpart DNA (pMHC) for effective activation.[28] For endogenous APCs, pMHC molecules containing identical peptide sequences are found clustered on the surface of APCs and lead to effective T cell activation.[52–54] Furthermore, effective nanocluster signaling has been shown to be necessary for T cell activation prior to the formation of supramolecular activation centers.[55]

In this systematic and quantitative analysis of aAPC particle size, we revealed the importance of designing cell-modulating nanoparticles with biology in mind. Here we considered both APC and T cell biology where primarily the field has been focusing on mimicking APCs. Furthermore, these mechanistic studies have implications for aAPC design for optimal therapeutic applications. One application is in utilizing the magnetic properties of the SPION aAPCs for magnetic enrichment of antigen-specific cells. Antigen-specific T cells occur at very low frequencies—at about 1 in every 10^5 to 10^6 T cells—and are therefore difficult to detect.[56] As immunotherapies have continued to develop, techniques surrounding identification and isolation of rare antigen-specific T cell have

grown in importance. Additionally, previous work has indicated that an enriched cell population can be activated to have therapeutic potential.[17] Therefore, aAPCs that are able to bind multiple TCRs may result in greater specificity and avidity and in greater enrichment of antigen-specific T cells. Our studies lay a foundation of quantitative analysis of particle aAPC size that pave the way for similar studies in the development of optimal aAPCs for magnetic enrichment.

Furthermore, these findings can provide aAPC design guidance in the in vivo activation of antigen-specific T cells. Using aAPCs to stimulate CD8+ T cells in vivo overcomes several challenges of the cancer immunity cycle and adoptive T cell transfer (ACT).[6,57] Endogenous APCs, such as dendritic cells (DCs), are immunosuppressed and can even be skewed to be immunosuppressive themselves.[58–60] This results in either deficient activation or immunosuppression of CD8+ T cells. Using aAPCs would bypass the need for DCs and allow effective and precise stimulation of antigen-specific CD8+ T cells. Additionally, in ACT, T cells are taken from a patient and cultured ex vivo then injected back into the body.[1] This process of ex vivo culture is time-consuming, technically challenging, and costly.[61–63] Therefore, in vivo activation of antigen-specific T cells is a primary goal of the field. Yet, achieving saturating conditions of 50 nm aAPCs in vivo may be impractical due to both poor nanoparticle-based biodistribution and retention and low frequency of antigen-specific T cells.[14,56] Thus, the goal is to engineer a particle that could achieve optimal biodistribution yet not require saturating amounts of aAPCs to activate a T cell. Our studies provide the basis for development of different sized biocompatible aAPCs to achieve robust in vivo immunotherapies.

In conclusion, we demonstrated how biologically inspired design of nanoparticle aAPCs to mimic a cell can lead to increased functionality of the particle and reveal aspects of cellular function. We utilized a reductionist approach to isolate the important properties of particle size and ligand density. Though we studied this in a model system with CD8+ T cells for immunotherapeutic applications, our findings and quantitative approach can impact and be implemented in other areas of cell modulation and mimicry.[14,64]

Supplementary Material

Refer to Web version on PubMed Central for supplementary material.

ACKNOWLEDGMENTS

J.W.H. thanks the NIH Cancer Nanotechnology Training Center at the Johns Hopkins Institute for NanoBioTechnology, the National Science Foundation Graduate Research Fellowship (DGE-1232825), and the ARCS foundation for fellowship support. The authors thank Michael Claiborne for his expertise and advice in experiments with early T cell signaling. The authors also thank John Michael McCaffery from the Integrated Imaging Center at Homewood and Barbara Smith and LaToya Roker from the Johns Hopkins School of Medicine Microscope Facility for assistance in the TEM imaging with T cells and aAPCs. This work was funded by support from the National Institutes of Health (P01-AI072677, R01-CA108835, R21-CA185819), TEDCO/Maryland Innovation Initiative, and the Coulter Foundation (JPS). Cell images in Figure 1a were reproduced under a Creative Commons License from Servier Medical Art (http://smart.servier.com/).

REFERENCES

(1). Rosenberg SA; Restifo NP; Yang JC; Morgan RA; Dudley ME Nat. Rev. Cancer 2008, 8, 299–308. [PubMed: 18354418]

(2). Della Bella S; Gennaro M; Vaccari M; Ferraris C; Nicola S; Riva A; Clerici M; Greco M; Villa M Br. J. Cancer 2003, 89, 1463–1472. [PubMed: 14562018]

(3). Satthaporn S; Robins A; Vassanasiri W; El-Sheemy M; Jibril JA; Clark D; Valerio D; Eremin O Cancer Immunol. Immunother. 2004, 53, 510–518. [PubMed: 14740176]

(4). Ye F; Yu Y; Hu Y; Lu W; Xie X J. Exp. Clin. Cancer Res. 2010, 29, 78. [PubMed: 20565840]

(5). Oelke M; Maus MV; Didiano D; June CH; Mackensen A; Schneck JP Nat. Med. 2003, 9, 619–625. [PubMed: 12704385]

(6). Chen DS; Mellman I Immunity 2013, 39, 1–10. [PubMed: 23890059]

(7). Perica K; Kosmides AK; Schneck JP Biochim. Biophys. Acta, Mol. Cell Res. 2015, 1853, 781–790.

(8). Fadel TR; Steenblock ER; Stern E; Li N; Wang X; Haller GL; Pfefferle LD; Fahmy TM Nano Lett. 2008, 8, 2070–2076. [PubMed: 18547120]

(9). Sunshine JC; Perica K; Schneck JP; Green JJ Biomaterials 2014, 35, 269–277. [PubMed: 24099710]

(10). Meyer RA; Sunshine JC; Perica K; Kosmides AK; Aje K; Schneck JP; Green JJ Small 2015, 11, 1519–1525. [PubMed: 25641795]

(11). Fadel TR; Sharp FA; Vudattu N; Ragheb R; Garyu J; Kim D; Hong E; Li N; Haller GL; Pfefferle LD Nat. Nanotechnol. 2014, 9, 639–647. [PubMed: 25086604]

(12). Steenblock ER; Fadel T; Labowsky M; Pober JS; Fahmy TM J. Biol. Chem. 2011, 286, 34883–34892. [PubMed: 21849500]

(13). Kosmides AK; Meyer RA; Hickey JW; Aje K; Cheung KN; Green JJ; Schneck JP Biomaterials 2017, 118, 16–26. [PubMed: 27940380]

(14). Hickey JW; Santos JL; Williford J-M; Mao H-Q J. Controlled Release 2015, 219, 536–547.

(15). Reddy ST; Van Der Vlies AJ; Simeoni E; Angeli V; Randolph GJ; O'Neil CP; Lee LK; Swartz MA; Hubbell JA Nat. Biotechnol. 2007, 25, 1159–1164. [PubMed: 17873867]

(16). Perrault SD; Walkey C; Jennings T; Fischer HC; Chan WC Nano Lett. 2009, 9, 1909–1915. [PubMed: 19344179]

(17). Perica K; Bieler JG; Schütz C; Varela JC; Douglass J; Skora A; Chiu YL; Oelke M; Kinzler K; Zhou S ACS Nano 2015, 9, 6861–6871. [PubMed: 26171764]

(18). Perica K; Tu A; Richter A; Bieler JG; Edidin M; Schneck JP ACS Nano 2014, 8, 2252–2260. [PubMed: 24564881]

(19). Tsai S; Shameli A; Yamanouchi J; Clemente-Casares X; Wang J; Serra P; Yang Y; Medarova Z; Moore A; Santamaria P Immunity 2010, 32, 568–580. [PubMed: 20381385]

(20). Singha S; Shao K; Yang Y; Clemente-Casares X; Solé P; Clemente A; Blanco J; Dai Q; Song F; Liu SW Nat. Nanotechnol. 2017, 12, 701. [PubMed: 28436959]

(21). Lillemeier BF; Mörtelmaier MA; Forstner MB; Huppa JB; Groves JT; Davis MM Nat. Immunol. 2010, 11, 90–96. [PubMed: 20010844]

(22). Molnár E; Swamy M; Holzer M; Beck-Garcia K; Worch R; Thiele C; Guigas G; Boye K; Luescher IF; Schwille P J. Biol. Chem. 2012, 287, 42664–42674. [PubMed: 23091059]

(23). Hwang J; Gheber LA; Margolis L; Edidin M Biophys. J. 1998, 74, 2184–2190. [PubMed: 9591645]

(24). Delcassian D; Depoil D; Rudnicka D; Liu M; Davis DM; Dustin ML; Dunlop IE Nano Lett. 2013, 13, 5608–5614. [PubMed: 24125583]

(25). Matic J; Deeg J; Scheffold A; Goldstein I; Spatz JP Nano Lett. 2013, 13, 5090–5097. [PubMed: 24111628]

(26). Deeg J; Axmann M; Matic J; Liapis A; Depoil D; Afrose J; Curado S; Dustin ML; Spatz JP Nano Lett. 2013, 13, 5619–5626. [PubMed: 24117051]

(27). Perica K; Medero ADL; Durai M; Chiu YL; Bieler JG; Sibener L; Niemöller M; Assenmacher M; Richter A; Edidin M Nanomedicine 2014, 10, 119–129. [PubMed: 23891987]

(28). Taylor MJ; Husain K; Gartner ZJ; Mayor S; Vale RD Cell 2017, 169, 108–119. [PubMed: 28340336]

(29). Ruvinsky I; Sharon N; Lerer T; Cohen H; Stolovich-Rain M; Nir T; Dor Y; Zisman P; Meyuhas O Genes Dev. 2005, 19, 2199–2211. [PubMed: 16166381]

(30). Turner MS; Kane LP; Morel PA J. Immunol. 2009, 183, 4895–4903. [PubMed: 19801514]

(31). Katzman SD; O'Gorman WE; Villarino AV; Gallo E; Friedman RS; Krummel MF; Nolan GP; Abbas AK Proc. Natl. Acad. Sci. U. S. A. 2010, 107, 18085–18090. [PubMed: 20921406]

(32). Zheng Y; Collins SL; Lutz MA; Allen AN; Kole TP; Zarek PE; Powell JD J. Immunol. 2007, 178, 2163–2170. [PubMed: 17277121]

(33). Zheng Y; Delgoffe GM; Meyer CF; Chan W; Powell JD J. Immunol. 2009, 183, 6095–6101. [PubMed: 19841171]

(34). Lanzavecchia A; Iezzi G; Viola A Cell 1999, 96, 1–4. [PubMed: 9989490]

(35). Ugel S; Zoso A; De Santo C; Li Y; Marigo I; Zanovello P; Scarselli E; Cipriani B; Oelke M; Schneck JP Cancer Res. 2009, 69, 9376–9384. [PubMed: 19934317]

(36). Sykulev Y; Brunmark A; TsoMIDES TJ; Kageyama S; Jackson M; Peterson PA; Eisen HN Proc. Natl. Acad. Sci. U. S. A. 1994, 91, 11487–11491. [PubMed: 7972089]

(37). Brower R; England R; Takeshita T; Kozlowski S; Margulies DH; Berzofsky JA; Delisi C Mol. Immunol. 1994, 31, 1285–1293. [PubMed: 7969189]

(38). Christinck ER; Luscher MA Nature 1991, 352, 67. [PubMed: 2062379]

(39). Demotz S; Grey HM; Sette A Science 1990, 249, 1028–1030. [PubMed: 2118680]

(40). Harding CV; Unanue ER Nature 1990, 346, 574. [PubMed: 2115981]

(41). Kimachi K; Croft M; Grey HM Eur. J. Immunol. 1997, 27, 3310–3317. [PubMed: 9464819]

(42). Purbhoo MA; Irvine DJ; Huppa JB; Davis MM Nat. Immunol. 2004, 5, 524. [PubMed: 15048111]

(43). Reay PA; Matsui K; Haase K; Wulfing C; Chien Y-H; Davis MM J. Immunol. 2000, 164, 5626–5634. [PubMed: 10820237]

(44). Sykulev Y; Joo M; Vturina I; Tsomides TJ; Eisen HN Immunity 1996, 4, 565–571. [PubMed: 8673703]

(45). Bray D; Levin MD; Morton-Firth CJ Nature 1998, 393, 85–88. [PubMed: 9590695]

(46). Fooksman DR; Grönvall GK; Tang Q; Edidin M J. Immunol. 2006, 176, 6673–6680. [PubMed: 16709826]

(47). Recouvreux P; Lenne P-F Curr. Opin. Cell Biol. 2016, 38, 18–23. [PubMed: 26829487]

(48). Aleksic M; Dushek O; Zhang H; Shenderov E; Chen J-L; Cerundolo V; Coombs D; van der Merwe PA Immunity 2010, 32, 163–174. [PubMed: 20137987]

(49). Huang J; Zarnitsyna VI; Liu B; Edwards LJ; Jiang N; Evavold BD; Zhu C Nature 2010, 464, 932–936. [PubMed: 20357766]

(50). Huppa JB; Axmann M; Mörtelmaier MA; Lillemeier BF; Newell EW; Brameshuber M; Klein LO; Schutz GJ; Davis MM Nature 2010, 463, 963–967. [PubMed: 20164930]

(51). Zhu C; Jiang N; Huang J; Zarnitsyna VI; Evavold BD Immunol. Rev. 2013, 251, 49–64. [PubMed: 23278740]

(52). Bosch B; Heipertz EL; Drake JR; Roche PA J. Biol. Chem. 2013, 288, 13236–13242. [PubMed: 23532855]

(53). Ferez M; Castro M; Alarcon B; van Santen HM J. Immunol. 2014, 192, 52–58. [PubMed: 24307729]

(54). Lu X; Gibbs JS; Hickman HD; David A; Dolan BP; Jin Y; Kranz DM; Bennink JR; Yewdell JW; Varma R Proc. Natl. Acad. Sci. U. S. A. 2012, 109, 15407–15412. [PubMed: 22949678]

(55). Lee K-H; Holdorf AD; Dustin ML; Chan AC; Allen PM ; Shaw AS Science 2002, 295, 1539–1542. [PubMed: 11859198]

(56). Jenkins MK; Moon JJ J. Immunol. 2012, 188, 4135–4140. [PubMed: 22517866]

(57). Restifo NP; Dudley ME; Rosenberg SA Nat. Rev. Immunol. 2012, 12, 269–281. [PubMed: 22437939]

(58). Hurwitz AA; Watkins SK Cancer Immunol. Immunother. 2012, 61, 289–293. [PubMed: 22237887]

(59). Ma Y; Shurin GV; Gutkin DW; Shurin MR Seminars in Cancer Biology; Elsevier, 2012; pp 298–306.

(60). Mosser DM; Edwards JP Nat. Rev. Immunol. 2008, 8, 958–969. [PubMed: 19029990]

(61). Chapuis AG; Ragnarsson GB; Nguyen HN; Chaney CN; Pufnock JS; Schmitt TM; Duerkopp N; Roberts IM; Pogosov GL; Ho WY Sci. Transl Med. 2013, 5, 174ra27–174ra27.

(62). Dudley ME; Wunderlich J; Nishimura MI; Yu D; Yang JC; Topalian SL; Schwartzentruber DJ; Hwu P; Marincola FM; Sherry R J. Immunother. 2001, 24, 363–373. [PubMed: 11565838]

(63). Mackensen A; Meidenbauer N; Vogl S; Laumer M; Berger J; Andreesen R J. Clin. Oncol. 2006, 24, 5060–5069. [PubMed: 17075125]

(64). Fang RH; Zhang L Annu. Rev. Chem. Biomol Eng. 2016, 7, 305–326. [PubMed: 27146556]

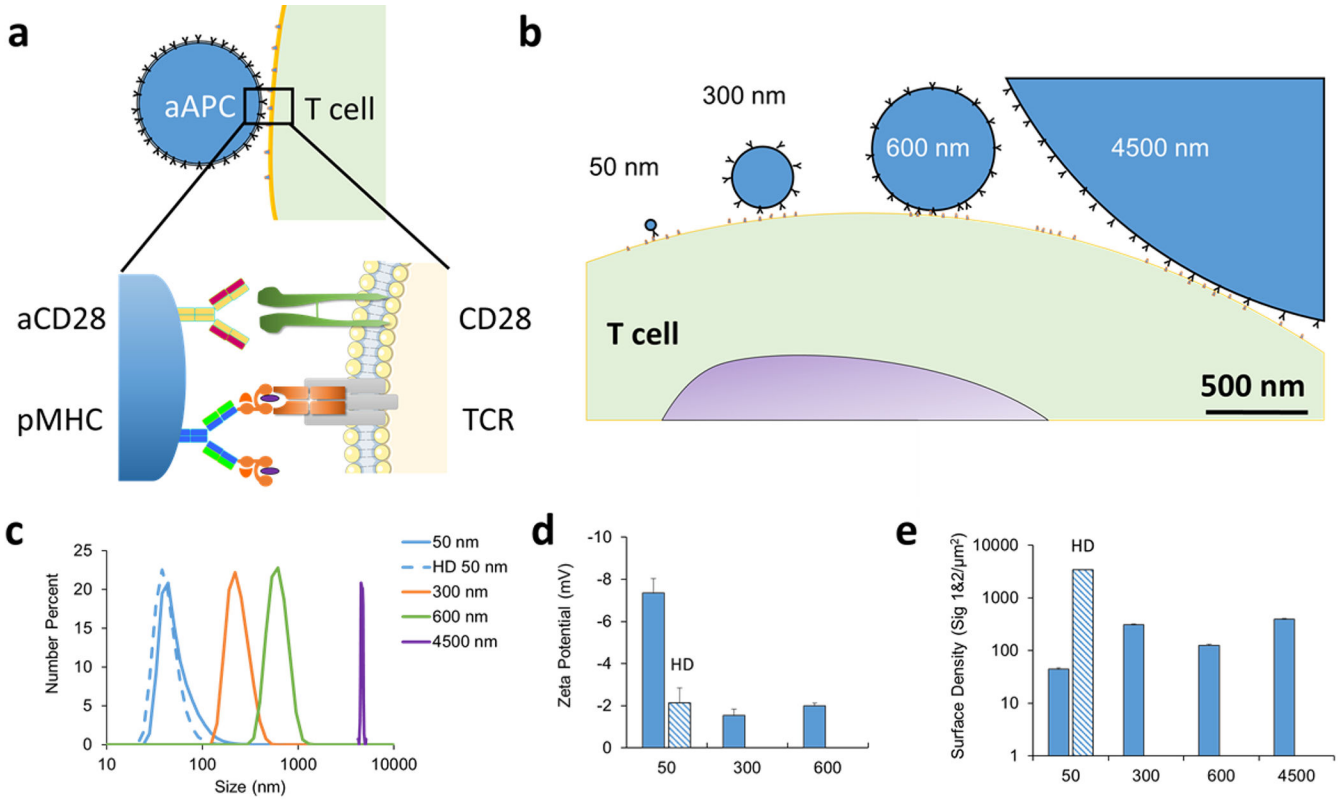

Figure 1.

Particle aAPCs are made with different sizes and ligand surface densities. (a) Schematic showing interaction between particle-based aAPC and cognate antigen-specific T cell. Stimulation is mediated through two signals. Signal 1 is antigen-specific and is between peptide loaded MHC-Ig (pMHC) and cognate TCR. Signal 2 is a costimulatory signal mediated between the binding of anti-CD28 and CD28 ligand on the T cell. (b) Schematic depicting relative sizes and ligand densities of aAPCs to a T cell. Scale bar = 500 nm. (c) Dynamic light scattering (DLS) measurements showing size distributions of nanoparticle aAPCs. 4500 nm aAPC particle size was analyzed by light microscopy. (d) Zeta potential measurements for different sized particles in PBS (error bars show s.e.m., $n = 3$). (e) The surface density of ligand defined as the number of Signal 1 and 2 molecules per μm^2 of the aAPC particle surface area, measured by fluorescent antibody detection (error bars show s.e.m., $n = 4$).

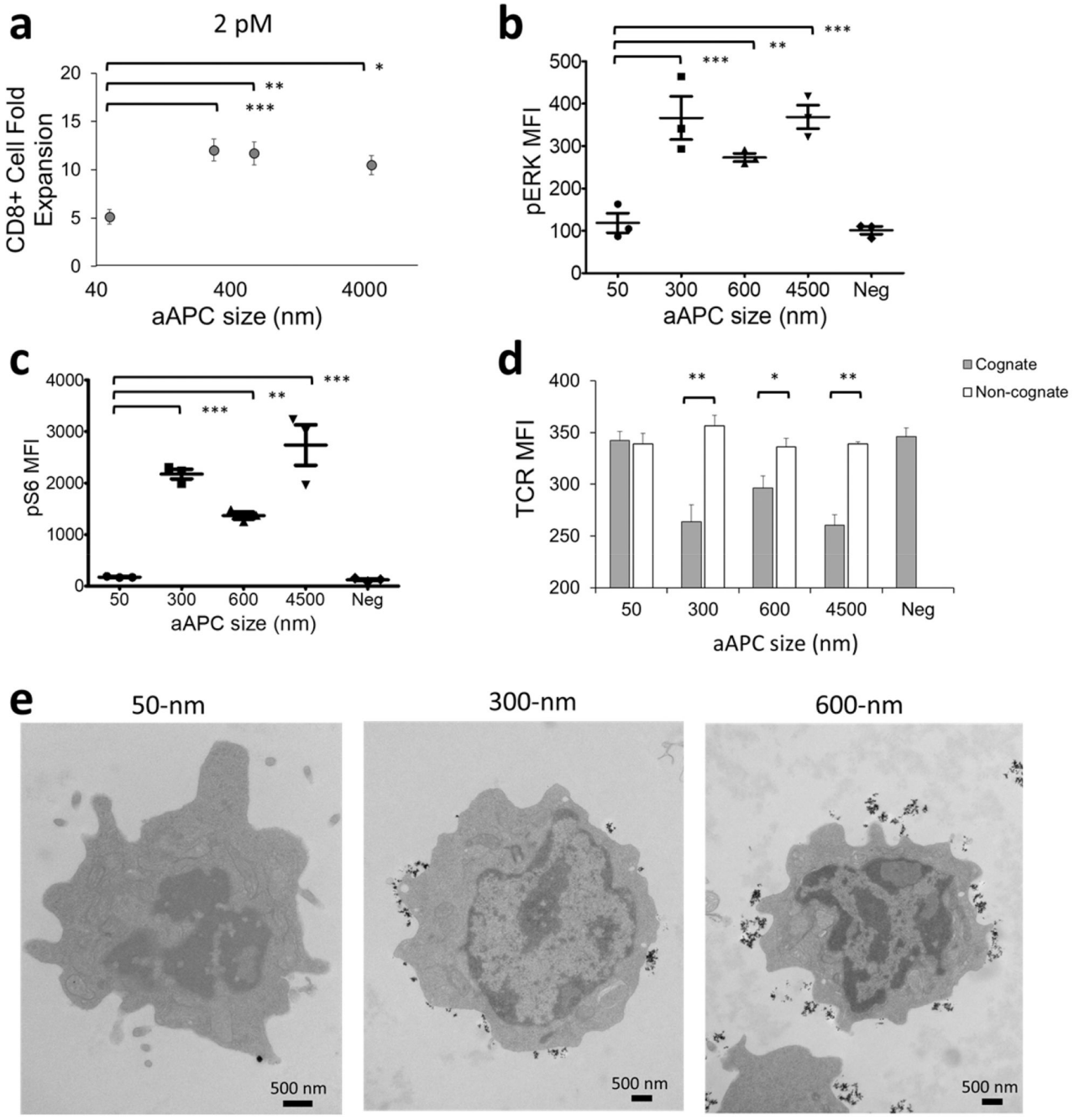

Figure 2.

Particle aAPC size influences the ability to activate CD8+ T cells. (a) Antigen-specific T cells are cultured with aAPCs at a controlled total dose of 2 pM conjugated pMHC, and fold proliferation is measured 7 days later (error bars show s.e.m.; ***$p < 0.0005$, **$p < 0.005$, *$p < 0.05$, $n = 9$, one-way ANOVA with Tukey's post test). (b-c) Mean fluorescent intensity (MFI) for (b) phosphorylated ERK and (c) phosphorylated ribosomal protein S6 of CD8+ T cells cultured with aAPCs at 37 °C for 30 min (error bars show s.e.m.; ***$p < 0.0005$, **$p < 0.005$, *$p < 0.05$, $n = 3$, one-way ANOVA with Dunnett's post test). (d) MFI for TCRβ of

CD8+ T cells cultured with aAPCs at 37 °C for 5 h (error bars show s.e.m.; $^{**}p < 0.005$, $^{*}p < 0.05$, $n = 3$, Student's t test). (e) Transmission electron microscopy (TEM) of 2C CD8+ T cells incubated with 50, 300, and 600 nm aAPCs for 1 h at 4 °C (scale bar = 500 nm).

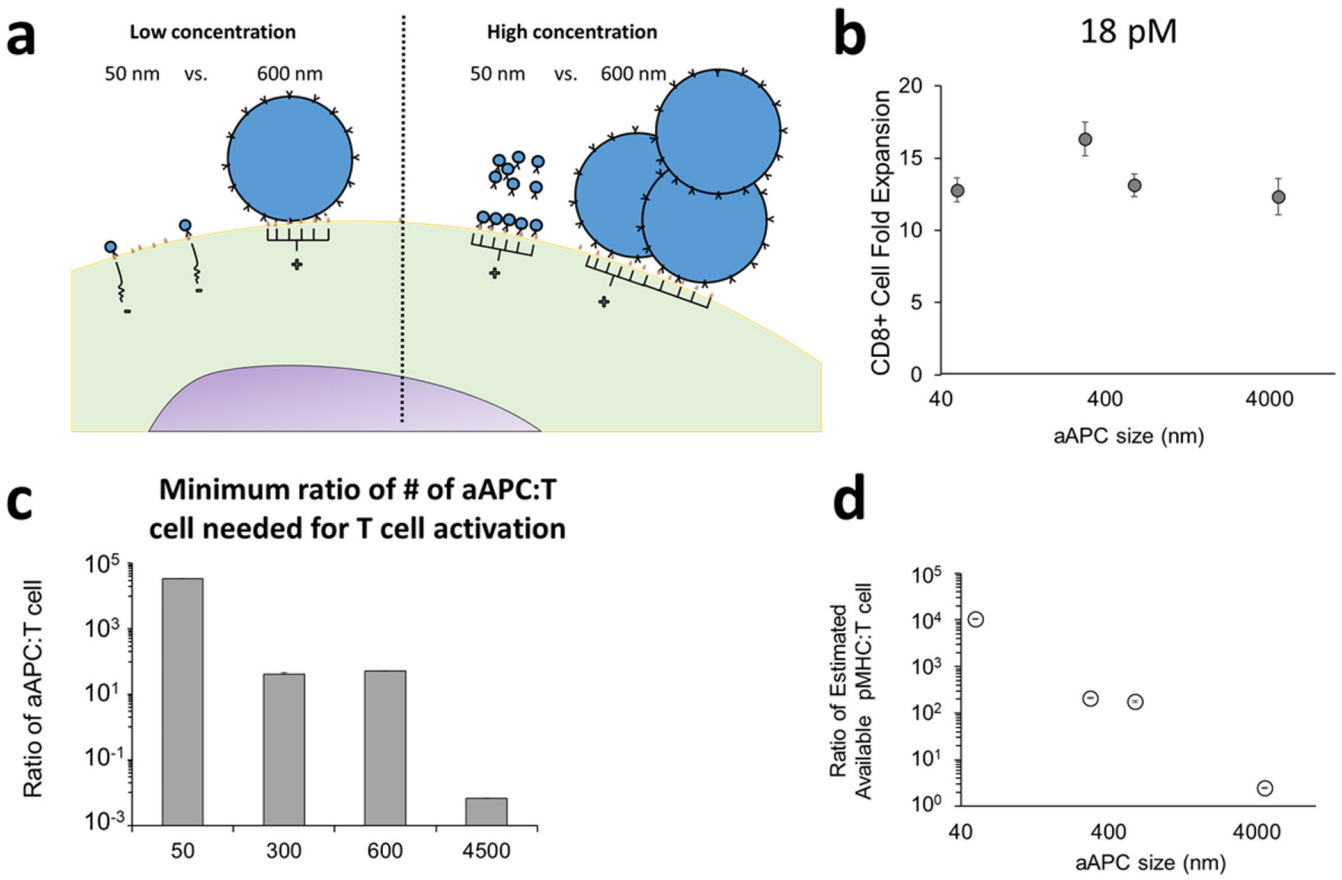

Figure 3.

Particle aAPC concentration reveals a saturating concentration of 50 nm aAPCs is needed to activate CD8+ T cells. (a) Schematic depicting hypothesis that saturating the T cell with 50 nm aAPCs is needed for the same nanoisland cluster-based activation as lower concentration larger 300 nm particles (600 nm aAPCs are depicted). (b) 18 pM dose of particle-conjugated pMHC is used to stimulate CD8+ T cells for 7 days, and the fold expansion is measured (no significant differences between aAPCs, one-way ANOVA, $n = 13$). (c-d) Dose-titrating amounts of particle aAPCs to activate T cells for 7 days determined lowest dose or (c) ratio of number of aAPCs to T cells or (d) estimated pMHC per T cell needed for activation (error bars show s.e.m., $n = 4$).

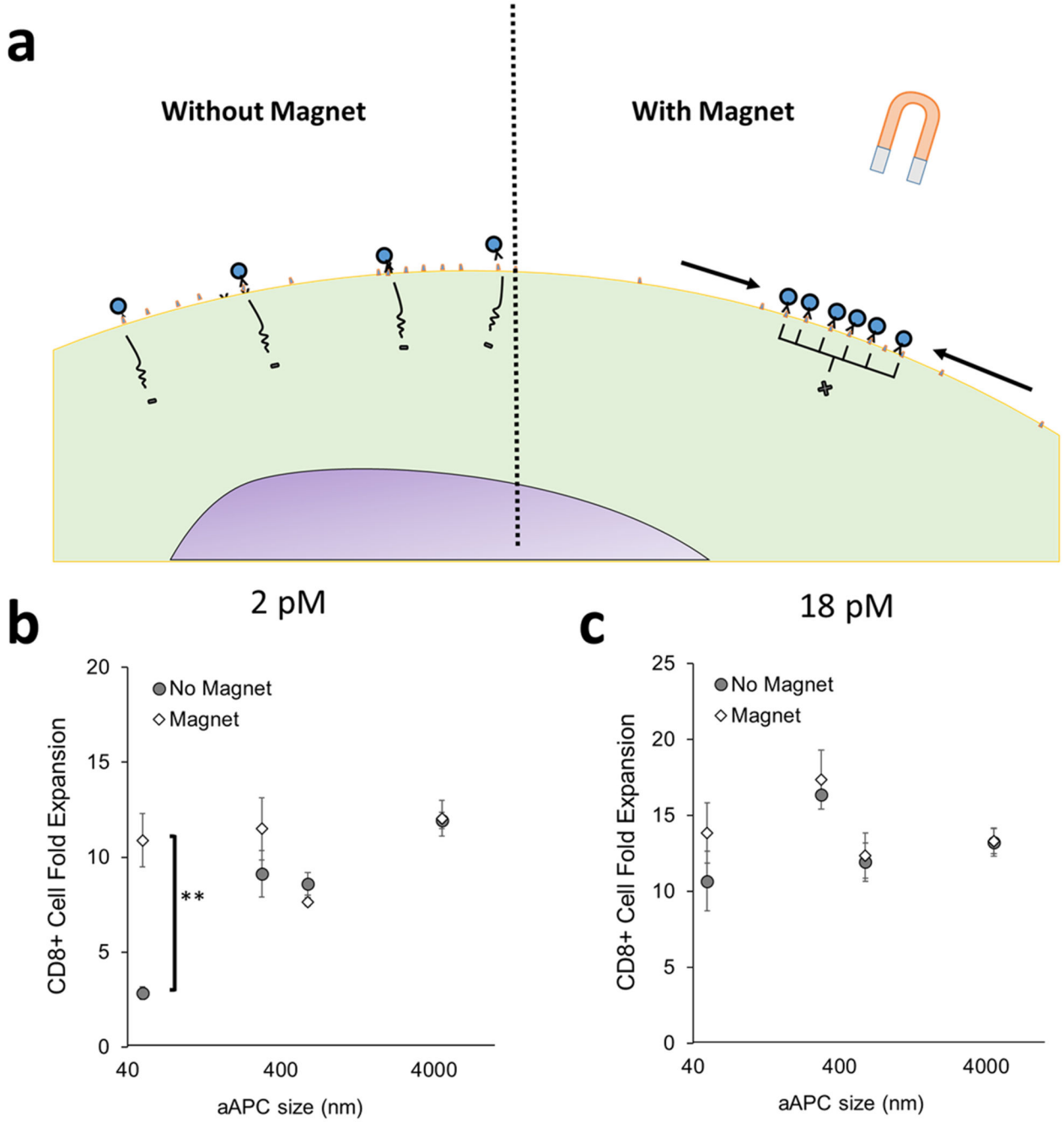

Figure 4.

Particle aAPC can be artificially magnetically clustered at subsaturating concentrations. (a) Schematic demonstrating the effect of magnetic fields on the 50 nm particle aAPCs to achieve artificial clustering. (b, c) CD8+ T cells and particle aAPCs were cultured for 7 days with or without the presence of a magnetic field and counted for fold expansion at either (b) 2 pM or (c) 18 pM dose of particle-conjugated pMHC (error bars show s.e.m.; $^{**}p < 0.005$, $n = 5–7$, Student's t test).

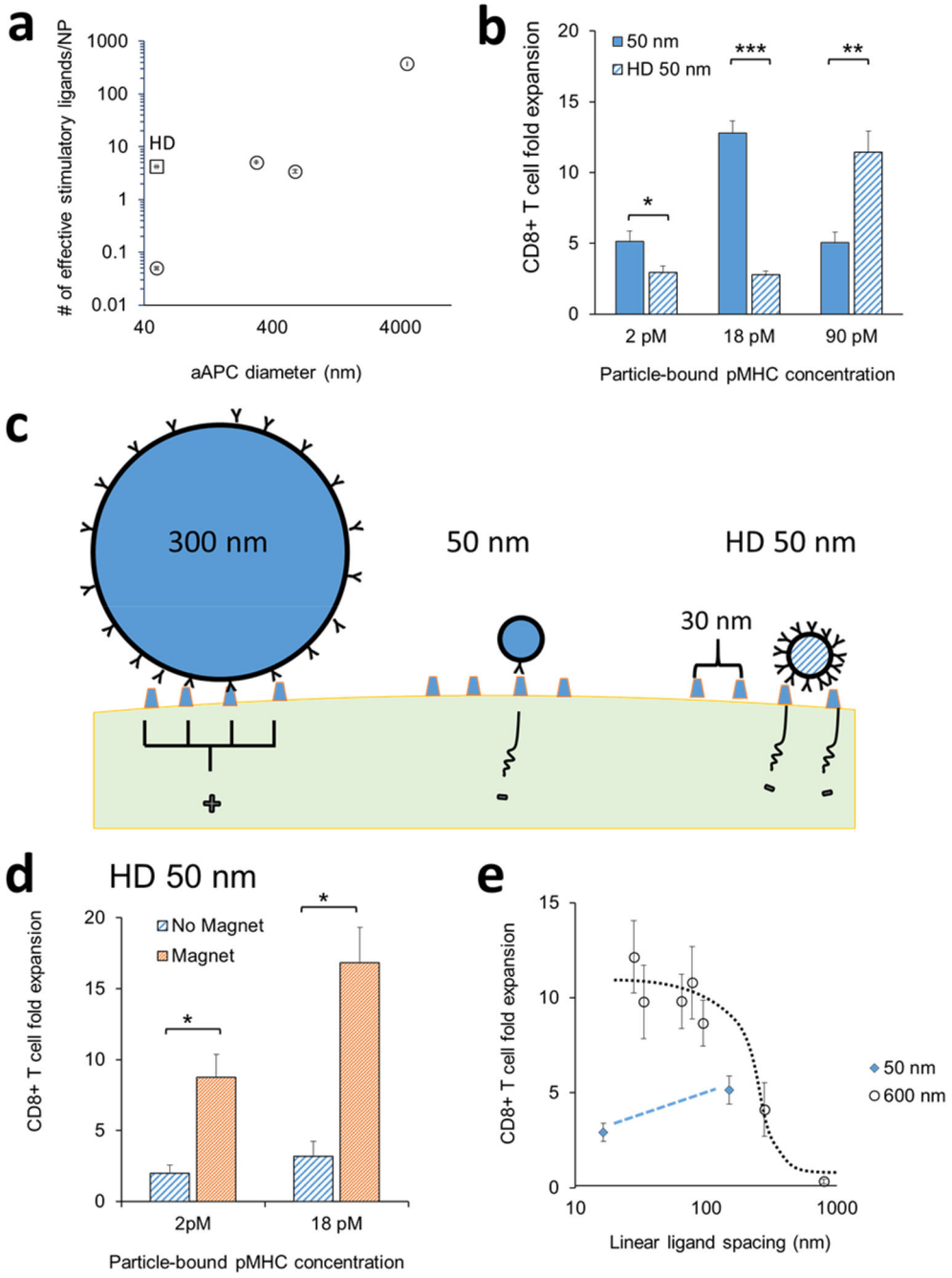

Figure 5.

Normalizing the effective available activating ligands does not overcome size-dependent stimulation capacity of aAPCs. (a) Calculated values of number of effective stimulatory ligands per particle. The square represents the HD 50 nm aAPCs made. (b) CD8+ T cells were incubated with equivalent doses of aAPC-bound pMHC of either 50 nm or HD 50 nm aAPCs for 7 days, and fold expansion was measured (error bars show s.e.m.; ***$p < 0.0005$, **$p < 0.005$, *$p < 0.05$, $n = 10–13$, Student's t test). (c) Schematic showing how aAPC size influences ligand-TCR interaction (spaced at ~30 nm) in TCR islands, where larger particles

facilitate more effective TCR ligand interactions, thus promoting T cell activation. (d) The effect of a magnetic field for either aAPC amounts at 2 pM or 18 pM of particle-bound pMHC (error bars show s.e.m.; $*p < 0.05$, $n = 5$, Student's t test). (e) 600 nm aAPCs with different ligand densities were incubated with T cells at 2 pM of particle-bound pMHC and fold expansion of CD8+ T cells was measured on day 7; 50 nm data replotted for comparison (error bars show s.e.m.; $n = 5$).